American Journal of Nanoscience and Nanotechnology
2013; 1(3): 74-78
Published online September 20, 2013 (http://www.sciencepublishinggroup.com/j/nano)
doi: 10.11648/j.nano.20130103.13

Effect of Nickel-alumina nanoparticle catalyst on the performance of methane steam reforming process

Aliasghar Rohani[1,*], Laleh Allahkaram[2], Ali Omidvar[3]

[1]Research institute of petroleum Industry, National Iranian Oil Company, Tehran, Iran
[2]Department of Chemistry, Islamic Azad University, Share Ray Branch, Tehran, Iran
[3]Department of Chemical Engineering, Islamic Azad University, Shahrood Branch, Shahrood, Iran

Email address:

Rohaniaa@ripi.ir (A. Rohani), laleh_allahkaram@yahoo.com(L. Allahkaram), aliomidvar60@yahoo.com (A. Omidvar)

To cite this article:

Aliasghar Rohani, Laleh Allahkaram, Ali Omidvar. Effect of Nickel-Alumina Nanoparticle Catalyst on the Performance of Methane Steam Reforming Process. *American Journal of Nanoscience and Nanotechnology.* Vol. 1, No. 3, 2013, pp. 74-78.
doi: 10.11648/j.nano.20130103.13

Abstract: In the present study, Fe-Mo/Al_2O_3 and Ni-Mo/Al_2O_3 catalysts were prepared using impregnation method. The structures of the catalysts were studied using XRD, BET and H_2-TPR techniques. Activities of both catalysts were investigated in a fixed-bed reactor for Methane Steam Reforming (MSR) reaction. The results indicated that Ni-Mo/Al_2O_3 catalyst system showed better activity and hydrogen yield for MSR reaction at normal operating conditions. The stability tests of both catalysts were examined at harsh operating condition which showed Ni-Mo/Al_2O_3 is a fairly stable catalyst. This study introduces a new catalyst, Ni-Mo/Al_2O_3, with high activity, stability for MSR reaction. The experimental evidence suggests that the main reason for the catalyst deactivation was sintering of the nickel particles.

Keywords: Catalyst, Fixed-Bed Reactor, Methane Steam Reforming, Alumina, Nano Particle

1. Introduction

Hydrogen has been widely used in the petro-chemical processes such as hydro-desulfurization, hydro-cracking, hydro-refining and so on. Nowadays, hydrogen becomes more and more involved as the feedstock in the synthesis of methanol/dimethyl ether (DME), and particularly, in the Fischer-Tropsch reactor to make liquid fuels from coal or natural gas. Besides, hydrogen serves as the ideal fuel for fuel cell, e.g., for proton exchange membrane (PEM) fuel cell [1-2]. Therefore, hydrogen is not only an important chemical feedstock, but also a clean energy carrier. The demand for low-cost hydrogen would be always predominant either for mass production or for distributed applications. However, hydrogen is known as an energy carrier not an energy source, which must be produced from other primary energy sources. The production of hydrogen from hydrocarbons, especially methane, i.e., the principal constituent of natural gas, can be performed in mainly three ways: steam reforming, partial oxidation, and auto thermal reforming [3]. It is acknowledged that steam reforming of methane is the most economical method for hydrogen production among the current commercial processes [4]. During the start-up procedure in MSR, steam alone can be possibly supplied into the reactor resulting in catalyst deactivation due to oxidation of metallic Ni [5, 6]. If methane alone is supplied into the reactor, there will be serious coke formation on the metallic Ni sites [7].However, the large-scale packed bed reactor with Ni catalyst supported on Al2O3 pellets suffers from the poor heat transfer behavior, which inevitably results in the large gradients in terms of temperature (and/or pressure) in axial and radial directions. As a consequence, the catalyst efficiency is reduced no matter how to improve the catalyst performance, for example, by adding promoters, such as Mo, P, CexZr1-xO2 [8-11]; or by changing supports, such as gadolinia doped ceria (GDC), ZrO2, ytria stabilized zirconia (YSZ) [12-14]. A major challenge is that Ni catalysts have a high thermodynamic potential for coke formation during reforming reactions, and several methods are discussed to synthesize coke resistant Ni catalysts [2, 15, 11]. Lercher et al. [17] reported that Pt/ZrO2 showed excellent performance in carbon dioxide reforming of methane (CDR). However, they have failed to apply Ni/ZrO2 with high Ni loading to the same reaction due to a serious plug of the reactor by coke formation. On the contrary, we have successfully performed CDR over Ni supported on ZrO2 and modiGed ZrO2 catalysts [18, 19]. Especially, a Ce–ZrO2 support is effective

to suppress coke formation. Consequently, Ni/Ce–ZrO2 exhibited high activity and stability in SMR [20, 21], oxy-reforming of methane (ORM) [22–24], and oxy-SMR (OSMR) [20, 19], owing to the ability to make mobile oxygen species, easier reducibility of Ce–ZrO2 and so on. Also, Montoya et al. [25] applied the Ni/Ce–ZrO2 system to CDR. However, Ni/Ce–ZrO2 is difficult to commercialize due to the high price of Ce–ZrO2 [7].

In the present study, the effect of Ni-promoted catalyst was studied in methane stream reforming for hydrogen production by adding Molybdenum. Ni-Mo catalysts based alumina was synthesized by impregnation method and characterized using XRD, BET and TPR. Then the catalyst activity and selectivity tests were performed in a fixed bed reactor. Finally this catalyst was compared with Fe-Mo/Al_2O_3 catalyst in MSR reaction.

2. Experimental

2.1. Catalyst Preparation

3 gram of $(NH_4)_6Mo_7O_{24}.4H_2O$ (Merck) was dissolved in one liter of distilled water. Then 11 grams of γ-Al_2O_3 (Nano Pars Spadana, 99% pure) was added to the solution. The solution was stirred by a high speed mechanical stirrer for 10 h, as molybdate anion was chemisorbed on the surface of γ-Al_2O_3 particles and Mo/Al_2O_3 catalyst was formed. The Fe-Mo/Al_2O_3 and Ni-Mo/Al_2O_3 catalysts were prepared by drop wise addition of Fe $(NO_3)_2.6H_2O$ (Merck Co., 99% pure) solution and Ni $(NO_3)_2.6H_2O$ (Merck Co., 99% pure) solution to Mo/Al_2O_3 slurry, respectively. Impregnated samples were subsequently air-dried at 323 K for 10 h and they were calcined in air at 923 K for 5 h.

2.2. Catalyst Characterization

The structures of these catalysts were studied using X-ray diffraction (XRD), which were obtained by a PW1840 X-ray powder diffractometer (Phillips, Netherland) using Cu tube anode operated at 40 kV and 30 mA with step size 0.02 from 5° to 90°. The specific surface areas of the samples were determined using the Brunauer–Emmett–Teller (BET) method with adsorption of nitrogen at liquid nitrogen temperature and subsequent desorption at room temperature after initial pre-treatment of the samples by degassing at 573 K for 1 h. The BET surface area was obtained with a Quanta Chrome Quantasorb surface area analyzer (USA).

Temperature programmed reduction (TPR) was conducted on a U-shaped quartz tube embedded in a programmable furnace. 80 mg of the catalyst was pre-treated with pure He flow at 573 K for 1 h and then reduced with a gas mixture flow (5% H2, 95% Ar, 40 ml/min). TPR patterns were obtained by using a recorder connected to a GC equipped with TCD in a temperature range 430–1250 K at a heating rate of 10 K/min.

2.2.1. RWGS Reactors System

The catalytic activity and stability tests of both catalysts were conducted in a fixed-bed reactor. A schematic diagram of the experimental apparatus and the configuration of the fixed-bed reactor are shown in Figure 1. The reaction tube (20mm ID and 150mm length) was made from stainless steel. The mass flow rate was controlled and measured using mass flow controllers (Hitachi). Steam in feed was produced by a steam generator (Arm field) at pressure of 4 bars. Prior to reaction, the catalyst was reduced in situ at 923 K for 4 h in 200 ml/min flow of hydrogen and nitrogen with hydrogen to nitrogen ratio of 1/5. A cold trap at the outlet of the reactor was used to condense out any water from the gas product stream. The water-gas shift reaction (WGS) is a chemical reaction in which carbon monoxide reacts with water vapor to form carbon dioxide and hydrogen:

$$CO\ (g) + H_2O\ (v) \rightarrow CO_2\ (g) + H_2\ (g) \qquad (1)$$

The water-gas shift reaction is an important industrial reaction.

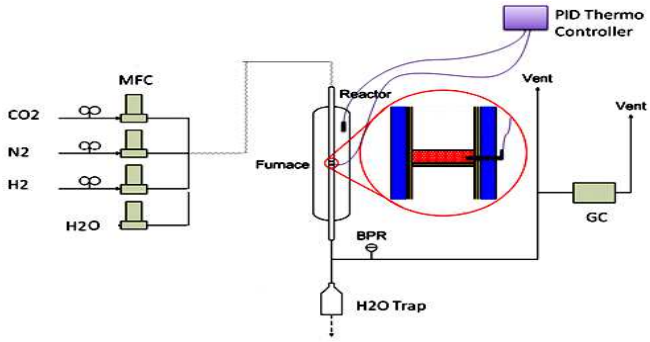

Figure 1. *A schematic diagram of the experimental apparatus of the fixed-bed reactor*

3. Results and Discussion

3.1. Textural Properties of Catalysts

Figure 2 shows the X-ray diffraction patterns for Ni-Mo/Al2O3 and Fe-Mo/Al2O3 catalyst systems. The active phases $Fe_2(MoO_4)_3$ and $NiMoO_4$ were identified in the X-ray diffraction patterns for Ni-Mo/Al2O3 and Fe-Mo/Al2O3 catalysts, respectively.

XRD Test

Powder XRD provides detailed information on the crystallographic structure and physical properties of materials and thin films. The sample is irradiated with a beam of monochromatic x-rays over a variable incident angle range. Interaction with atoms in the sample results in diffracted x-rays when the Bragg equation is satisfied. Resulting spectra are characteristic of chemical composition and phase. The technique uniquely provides phase identification (e.g. graphite or diamond), along with phase quantification, % crystallinity, crystallite size and unit cell size. English physicists Sir W.H. Bragg and his son

Sir W.L. Bragg developed a relationship in 1913 to explain why the cleavage faces of crystals appear to reflect X-ray beams at certain angles of incidence (theta θ). The variable *d* is the distance between atomic layers in a crystal, and the variable lambda l is the wavelength of the incident X-ray beam; n is an integer. This observation is an example of X-ray wave interference, commonly known as X-ray diffraction (XRD), and was direct evidence for the periodic atomic structure of crystals postulated for several centuries. ($n\lambda = 2d \sin\theta$)

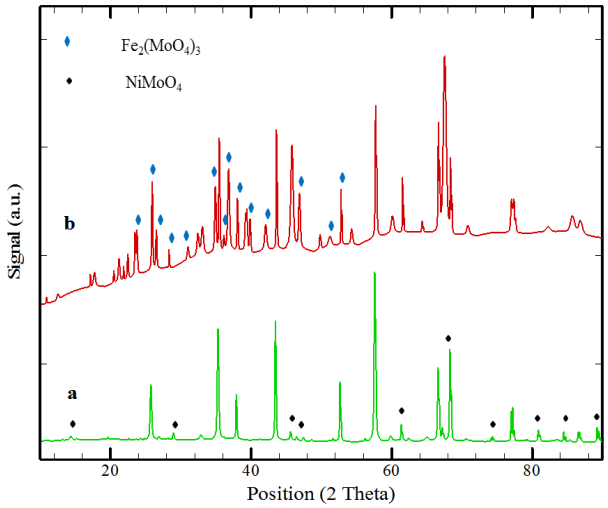

Figure 2. *The XRD patterns for (a) Ni-Mo/Al2O3 and (b) Fe-Mo/Al2O3 catalysts.*

The metals concentrations, BET surface areas and average pore diameters of both catalysts are shown in Table 1. Textural and compositional properties of catalysts are similar because the preparation method and concentrations are the same.

Table 1. *Specific surface area and mass percent of metals for each catalyst*

Catalyst	Specific surface area (m^2/g)	Average pore diameter (nm)	%Mo	%Ni	%Fe
Ni-Mo	67	16	11.9	7.4	-
Fe-Mo	69	17	12.3	-	7.1

Temperature programmed reduction (H_2-TPR) was carried out to investigate the reducibility of the Ni-Mo/Al_2O_3 and Fe–Mo/Al_2O_3. The H_2 –TPR pattern of catalysts are shown in Figure 3. It is clear that active phase significantly affects the reduction behaviour of the Fe-Mo/Al_2O_3 and Ni-Mo/Al_2O_3 catalysts. $Fe_2(MoO_4)_3$ Existence in structure of Fe-Mo/Al_2O_3 decreases catalyst reducibility and $NiMoO_4$ Existence in structure of Ni-Mo/Al_2O_3 improve reducibility of catalyst.

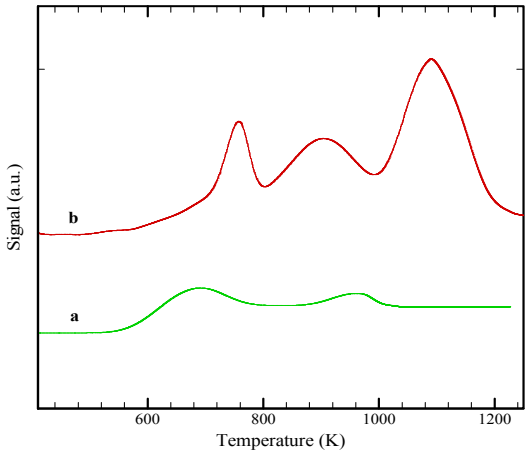

Figure 3. *The H_2-TPR patterns for Ni-Mo/Al_2O_3 (a) and Fe-Mo/Al_2O_3 (b) catalysts.*

3.2. Catalytic Activity and Selectivity

Activity of the Ni-Mo/Al2O3 catalyst system is compared to Fe-Mo/Al2O3 catalyst system in a fixed bed reactor, as shown in figure 4. The same feed composition and space velocity was used for both catalysts (400 ml/min, Steam/Methane = 0.5). It can be seen that the Ni-Mo/Al2O3 catalyst has higher methane conversion than Fe-Mo/Al2O3. The conversion of methane increased with the reaction temperature as it increased from 673 to 973 K.

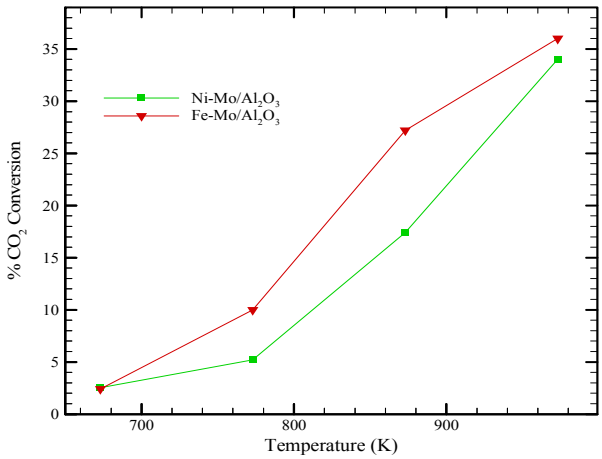

Figure 4. *Co_2 conversion versus temperature for both catalyst systems (S/C= 0.5, and Space Velocity = 400 ml/min Catalyst loading= 3g).*

Figure 5 shows hydrogen yields versus time at 873 K for both catalysts. As it is shown, the hydrogen yield for Ni-Mo/Al2O3 catalyst is higher than that of Fe-Mo/Al2O3. It is also apparent that the hydrogen yield for Ni-Mo/Al2O3 catalyst is higher than those of Fe-Mo/Al2O3 catalyst at low temperature; however they have same yield at high temperature (above 973 K). Hydrogen yield is defined as follows. Hydrogen yield= Moles of generated H2 / (Moles of generated CO + Moles of generated H2)

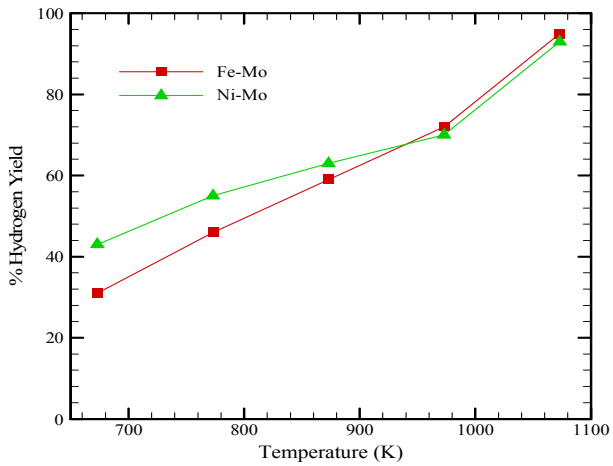

Figure 5. *Hydrogen yields versus temperature for both catalysts (S/C= 0.5, and Space Velocity = 400 ml/min, Catalyst loading= 5g).*

Figure 6 illustrates the dependence of methane conversion on the mole fraction of H2O in the H2O/CH4 feed. With increasing H2O concentration, methane conversion for Ni-Mo/Al2O3 catalyst passes over a volcano showing the maximum value at H2O/CH4 = 0.5. The behavior is quite different for Fe-Mo/Al2O3 catalyst system. The methane conversion slowly decreased as mole% of H2O increased.

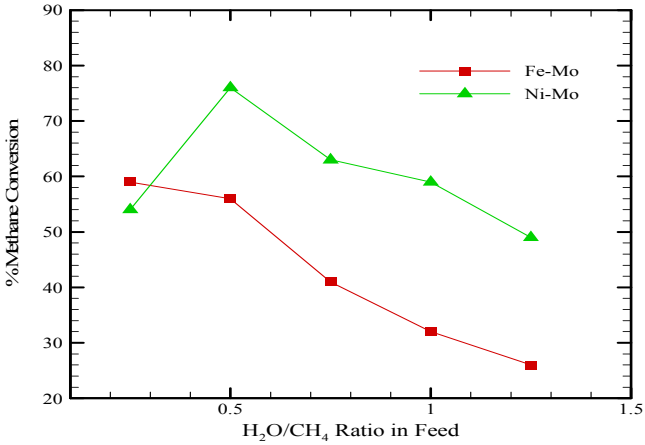

Figure 6. *Methane conversion versus temperature for both catalysts (Space Velocity = 400 ml/min, Catalyst loading= 5g T=873K).*

The respective contributions of Reverse Water Gas Shift and steam reforming reactions as a function of temperature and CH4/CO2 ratio were evaluated by measuring the H2O concentration in the products (Fig. 7). Irrespective of the feed composition it can be observed that H2O concentration increases with increasing temperature until reaching a maximum value and then decreases at higher temperatures. At low temperatures, the increase in H2O concentration can be attributed to the increasing contribution of RWGS reaction without significant influence of steam reforming. As temperature increases, the reaction rate of steam reforming increases more than RWGS, which leads to an increasing consumption of H2O and causes the observed maximum and then the decrease in H2O concentration with increasing temperatures. This effect is more pronounced at high CH4 concentration. This is expected since steam reforming rate depends on CH4 concentration. Interestingly, steam reforming reaction is faster than RWGS for CH4/CO2 = 2 at 800 C. Water is then consumed as it is formed and the overall process can be described by CO2 reforming only. As a result H2/ CO are highest, being equal to unity.

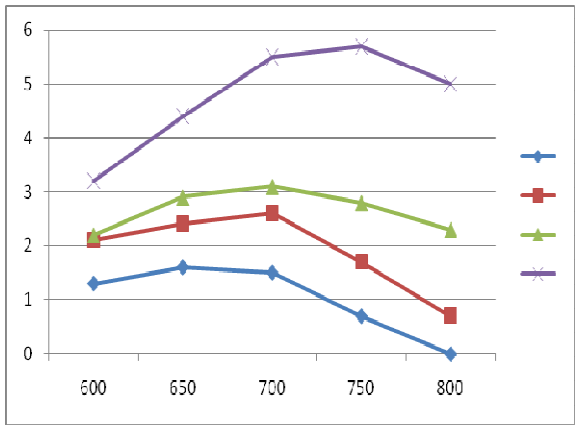

Figure 7. *Influence of the temperature on the formation of H_2O at different ratio of CH4/CO2*

3.3. Stability Tests

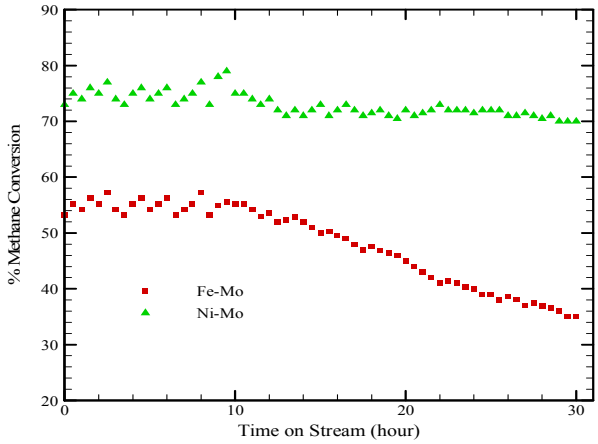

Figure 8. *Stability of both catalyst systems for MSR reaction with versus time on stream (S/C= 0.5, Space Velocity= 400 ml/min, Catalyst loading= 3g, T=873 K)*

The time-on-stream (TOS) analysis of the activity for the MSR reaction was carried out for a continuous period of 30 h for both catalyst systems. The results of TOS analysis are shown in figure 8. It was evident that The Fe-Mo/Al2O3 was gradually deactivated after 10 h of reaction time. The Ni-Mo/Al2O3 catalyst was stable through 30 h of reaction time.

4. Conclusions

In comparison of both catalyst systems, Ni-Mo/Al2O3 catalyst system showed better activity and hydrogen yield for MSR reaction at normal operating conditions. This catalyst had maximum methane conversion when H2O/CH4 in feed is equal to 0.5. The stability tests of both catalysts

were examined at harsh operating condition which showed Ni-Mo/Al2O3 is a fairly stable catalyst. This study introduces Ni-Mo/Al2O3 as a new catalyst with high methane conversion and acceptable hydrogen yield.

References

[1] Rostrup-Nielsen "JR. Catal. Rev", 2004, pp.247-70.

[2] Xuli Zhai, Yinhong Cheng, Zhongtao Zhang, Yong Jin, Yi Cheng, "International journal of hydrogen energy" , 2011, pp.7105-7113.

[3] Ismagilov Z.R., Pushkarev V.V., Podyacheva O.Y., Koryabkina N.A., Veringa H. A., "Chem Eng J ",2001 pp.355-60.

[4] Mustafa B. "Int J Hydrogen Energy ",2008, pp.4013-29.

[5] Rostrup-Nielsen JR. In: Anderson JR, Boudart M, editors. "Catalysis, science and technology", vol. 5. Berlin: Springer, 1984, p.1.

[6] Ridler DE, Twigg MV. In: Twigg MV, editor. Catalyst handbook (2nd ed.). England: "Wolfe Publishing Ltd",1989, p. 225 [chapter 5].

[7] Young-Sam Oh, Hyun-Seog Roh, Ki-Won Jun b, Young-Soon Baek, "International Journal of Hydrogen Energy", 28 (2003) ,pp.1387–1392.

[8] Kepinski L, Stasinska B, Borowiecki T. "Carbon "2000, 38, pp. 1845-56.

[9] Xu J, Chen LW, Tan KF, Borgna A, Saeys M.," J. Catal ", 2009, 261, pp.158-65.

[10] Wang K, Li XJ, Ji SF, Shi XJ, Tang JJ., "Energy Fuels", 2009, pp.25-31: 23.

[11] Oh YS, Roh HS, Jun KW, Baek YS. "Int J Hydrogen Energy", 2003, pp.1387-92: 28.

[12] Huang TJ, Huang MC., "Chem Eng J "2008, pp.149-53: 145.

[13] Nguyen LQ, Abella LC, Gallardo SM, Hinode H." React Kinet Catal Lett", 2008, pp. 227-32: 93.

[14] Wang Y, Yoshiba F, Kawase M, Watanabe T." Int J Hydrogen Energy" 2009, pp.3885-93: 34.

[15] Liu CJ, Ye JY, Jiang JJ, Pan YX. "ChemCatChem", 2011, pp.529-41: 3.

[16] Liu CJ, Burghaus U, Besenbacher F, Wang ZL. 'ACS Nano" 2010, pp.5517-26: 4.

[17] Lercher JA, Bitter JH, Hally W, Niessen W, Seshan K." Stud Surf Sci Catal "1996, pp.463: 101.

[18] Li X, Chang J-S, Park S-E. "Chem Lett ", 1999, pp.1099.

[19] Li X, Chang J-S, Tian M, Park S-E." Appl Organometal Chem "2001, pp.109: 15.

[20] Roh H-S, Jun K-W, Dong W-S, Park S-E, Baek Y-S." Catal Lett" 2001, p31: 74.

[21] Roh H-S, Jun K-W, Dong W-S, Chang J-S, Park S-E, Joe Y-I. "J Mol Catal A" 2002, p.1137: 18.

[22] Roh H-S, Dong W-S, Jun K-W, Park S-E. "Chem Lett "2001, p.88.

[23] Dong W-S, Jun K-W, Roh H-S, Liu Z-W, Park S-E. "Catal Lett "2002, p.78: 215.

[24] Dong W-S, Roh H-S, Jun K-W, Park S-E, Oh Y-S. "Appl Catal A "2002, p.63: 226.

[25] Montoya JA, Romero-Pascual E, Gimon C, Del Angel P, Monzon A. "Catal Today "2000, p.71: 63.